Journal of Molecular Catalysis A: Chemical 304 (2009) 16–21

Contents lists available at ScienceDirect

Journal of Molecular Catalysis A: Chemical

journal homepage: www.elsevier.com/locate/molcata

# Adsorption and reaction of $Mo(CO)_6$ on chemically modified Pt(1 1 0) model surfaces

Zhiquan Jiang[a,*], Lingshun Xu[b], Weixin Huang[a,b,**]

[a] Hefei National Laboratory for Physical Sciences at the Microscale, University of Science and Technology of China, 96 Jinzhai Road, Hefei 230026, Anhui, China
[b] Department of Chemical Physics, University of Science and Technology of China, Hefei 230026, China

ARTICLE INFO

*Article history:*
Received 15 October 2008
Received in revised form 18 December 2008
Accepted 10 January 2009
Available online 20 January 2009

*Keywords:*
Molybdenum hexacarbonyl
Pt(1 1 0)
Mo/Pt(1 1 0)
$MoO_x$/Pt(1 1 0)
High-resolution electron energy loss spectroscopy
Thermal desorption spectroscopy

ABSTRACT

The surface chemistry of $Mo(CO)_6$ on Pt(1 1 0), Mo/Pt(1 1 0) and $MoO_x$/Pt(1 1 0) surfaces was investigated by high-resolution electron energy loss spectroscopy and thermal desorption spectroscopy. The Mo/Pt(1 1 0) surface was prepared by dosing $Mo(CO)_6$ on Pt(1 1 0) at 700 K followed by annealing at 1000 K. The oxidation of Mo/Pt(1 1 0) surface leads to the formation of $MoO_x$/Pt(1 1 0) surface. $Mo(CO)_6$ molecularly chemisorbs on the clean Pt(1 1 0) and $MoO_x$/Pt(1 1 0) surfaces at 100 K, however, undergoes partial dissociation on the Mo/Pt(1 1 0) surface. The Mo/Pt(1 1 0) surface more strongly donates electrons to adsorbates than the Pt(1 1 0) and $MoO_x$/Pt(1 1 0) surfaces, and thus exhibits a higher reactivity toward $Mo(CO)_6$. We propose that the interaction of CO ligands in $Mo(CO)_6$ with the metal surface determines the adsorption behavior of $Mo(CO)_6$. Our work enriches the surface chemistry of $Mo(CO)_6$ on metallic substrates.



## 1. Introduction

The adsorption and reactivity of organometallic compounds on catalyst surfaces have recently attracted increasing attention. Group VIB hexacarbonyls render themselves suitable as precursors for selective metal deposition on surfaces, providing an effective approach to prepare supported metal catalysts [1,2]. The metals in the carbonyls are normally in the zero-valent state and the CO ligands are stable, noncondensable gas, therefore, thermal decomposition of metal carbonyls can, in principle, eliminate CO from the carbonyl molecules and thus deposit the metal on the surface. Thermal decomposition of $W(CO)_6$ [3,4] and $Fe(CO)_5$ [4–8] has been investigated and subsequently mechanistic studies of the thermal decomposition was in connection with chemical vapor deposition processes. Employing these metal carbonyls as the precursor, the metallic components can be deposited on substrates.

$Mo(CO)_6$ is usually used as an effective metal-containing precursor for the preparation of the molybdenum species in heterogeneous catalysis [4,9–13]. Therefore, it is very meaningful to investigate the adsorption and decomposition of $Mo(CO)_6$ on various substrates, and to acquire a thorough comprehension of the mechanism of chemisorption and thermal decomposition of $Mo(CO)_6$. So far, the adsorption and reaction of molybdenum hexacarbonyl have been extensively investigated on catalyst supports, such as silica [14,15], γ-alumina [16,17] and alumina thin films [18–25]. This can provide insights into fabrication of real catalysts modified by molybdenum species. Chemisorption of $Mo(CO)_6$ are primarily dependent on chemical properties of substrates. The dissociative adsorption of $Mo(CO)_6$ occurred on Rh(1 0 0) [26,27] whereas molecular adsorption of $Mo(CO)_6$ occurred on graphite and Ag(1 1 1) surfaces [28]. Chemical modification of surfaces has been shown to influence photodecomposition of metal carbonyls considerably by altering both electronic and physical natures of substrate surfaces [29–31]. $Mo(CO)_6$ adsorbed dissociatively on Ru(0 0 1) surface, but chemical modifications of the surface by O- and S-adatoms could substantially stabilize the $Mo(CO)_6$ adsorbate and thus suppress the decomposition [29]. It was reported that $Mo(CO)_6$ molecularly and dissociatively chemisorbed on the clean and K-modified Cu(1 1 1) surfaces, respectively [30]. A complete molecular adsorption of $Mo(CO)_6$ occurred on clean Si(1 1 1)-7 × 7 whereas the partial dissociation was observed on K-preadsorbed Si(1 1 1)-7 × 7, which was attributed to an increase of the surface electron density of Si(1 1 1) by potassium [32]. Moreover, the extent of dissociation was found to depend on the potassium coverage, and

* Corresponding author. Tel.: +86 551 3600435; fax: +86 551 3600437.
** Corresponding author at: Hefei National Laboratory for Physical Sciences at the Microscale, University of Science and Technology of China, 96 Jinzhai Road, Hefei 230026, Anhui, China. Tel.: +86 551 3600435; fax: +86 551 3600437.
*E-mail addresses:* jzhiquan@ustc.edu.cn (Z. Jiang), huangwx@ustc.edu.cn (W. Huang).

1381-1169/$ – see front matter © 2009 Elsevier B.V. All rights reserved.
doi:10.1016/j.molcata.2009.01.012

a high potassium coverage resulted in a large fraction of dissociation [30]. Meanwhile, coadsorption of potassium was also observed to significantly enhance the photodissociation of $Mo(CO)_6$ adsorbed on Cu(1 1 1) and Si(1 1 1)-7 × 7 by opening a completely different photodissociation channel that became energetically possible due to substantial decreases in the work function [33].

In a preceding paper [13] metallic molybdenum was deposited on platinum substrates via thermal decomposition of $Mo(CO)_6$ and subsequent annealing at high temperatures, without any carbon and oxygen contaminants. The surface chemistry of metal carbonyls was also studied on platinum surfaces by Zaera [6]. In this paper, $Mo(CO)_6$ adsorption was comparatively investigated on clean, Mo-modified and $MoO_x$-modified Pt(1 1 0) surfaces. We found that $Mo(CO)_6$ molecularly adsorbs on the clean Pt(1 1 0) and $MoO_x$/Pt(1 1 0) surfaces but partially dissociates on the Mo/Pt(1 1 0) alloy surface. The modification of Pt(1 1 0) by metallic molybdenum is responsible for the observed enhanced reactivity toward $Mo(CO)_6$. The oxidation of Mo into $MoO_x$ hinders the Mo–Pt interaction, causing $MoO_x$/Pt(1 1 0) more inert than Mo/Pt(1 1 0). Our work enriches the surface chemistry of $Mo(CO)_6$ on metallic substrates.

## 2. Experimental

Experiments were carried out in an ultrahigh vacuum (UHV) system with a base pressure of $2.0 \times 10^{-10}$ mbar, which was described in detail elsewhere [12,13,34,35]. In brief, the UHV system was equipped with facilities for Auger electron spectroscopy (AES), X-ray photoelectron spectroscopy (XPS), high-resolution electron energy loss spectroscopy (HREELS), and thermal desorption spectroscopy (TDS) experiments. The AE spectra were recorded through a hemispherical energy analyzer, with an incident electron energy of 3 keV at a pass energy of 150 eV. The XP spectra were taken with Mg Kα radiation (1253.6 eV) at a pass energy of 50 eV. The HREEL spectra were collected on an ELS-22 instrument in the specular direction, with an incident angle of 60° and a primary incident electron beam energy of 5.0 eV. In this paper, the vibrational frequencies were all expressed in the unit of $cm^{-1}$ (1 meV = 8 $cm^{-1}$). The spectral resolution was approximately 100 $cm^{-1}$ on a clean surface. In the TDS experiments, the sample was heated at a rate of 8 K/s. In order to avoid the signal from the back of the sample, it was positioned at about 3 mm away from the collector of mass spectrometer, which was fixed on the inner wall of the flange. The filament of the mass spectrometer is far behind the collector, and the adsorbates do not suffer severe electron beam decomposition induced by electrons from the ionizer of the mass spectrometer. A Pt(1 1 0) single crystal was fixed on the sample holder with Ta wires, and the temperature was monitored by a chromel–alumel thermocouple spot-welded on the back side of the sample. The sample could be either cooled down to 100 K with liquid nitrogen, or resistively heated up to 1200 K. The Pt(1 1 0) surface was cleaned by standard procedures, including oxidation, $Ar^+$ sputtering and annealing at a high temperature, until no contaminants could be detected by AES. Prior to the experiments, $Mo(CO)_6$ was purified in the manifold via several freeze–pump–thaw cycles. $Mo(CO)_6$ was fed through a capillary array doser, which was positioned directly in front of the sample, thus preventing an undesirable rise in the background pressure of $Mo(CO)_6$. The exposure was determined by integrating the pressure increase as a function of time, without correction for the local dose enhancement and gauge sensitivity. All exposures determined in this way were specified hereafter as Langmuirs (1 L = $1.0 \times 10^{-6}$ Torr s).

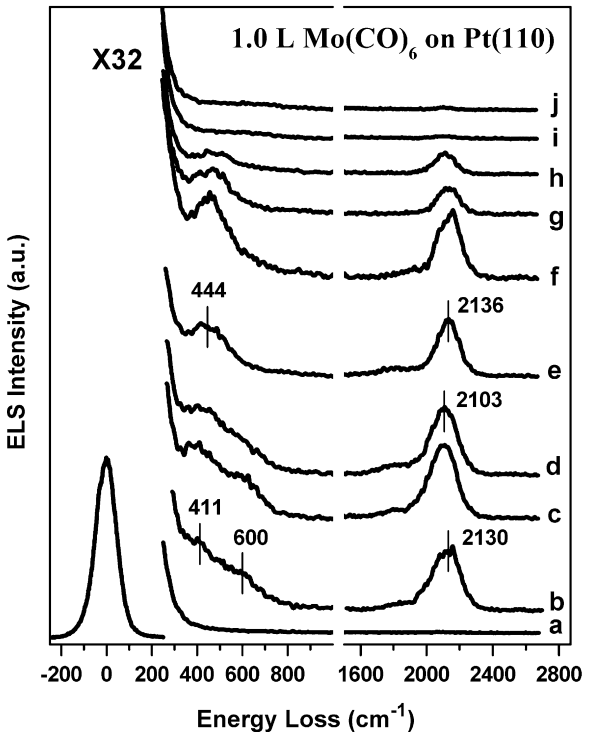


**Fig. 1.** HREEL spectra of (a) a clean Pt(1 1 0) surface at 100 K, then (b) exposed to 1.0 L $Mo(CO)_6$ at 100 K and subsequently annealed at (c) 150 K, (d) 200 K, (e) 250 K, (f) 300 K, (g) 400 K, (h) 500 K, (i) 600 K, and (j) 700 K.

## 3. Results and discussion

Experiments of $Mo(CO)_6$ adsorption were all performed at cryogenic temperatures because of the low sticking coefficient of $Mo(CO)_6$ on solid surfaces at room temperature. Our previous TDS and XPS results of $Mo(CO)_6$ on Pt(1 1 0) showed that $Mo(CO)_6$ adsorbed molecularly on the surface at 100 K; most of the adsorbates desorbed molecularly from the substrate upon annealing, and the remainder underwent thermal decomposition with further increasing sample temperature [13]. Fig. 1 displays a series of HREEL spectra of $Mo(CO)_6$ with an exposure of 1.0 L adsorbed on a clean Pt(1 1 0) surface at 100 K and subsequently annealed to the indicated temperatures. The exposure of 1.0 L $Mo(CO)_6$ on clean Pt(1 1 0) gives rise to an intense signal at 2130 $cm^{-1}$ and 2 relatively weak vibrations at 411 and 600 $cm^{-1}$ in the HREELS. These peaks could be assigned to the C–O stretching ($\nu_6$), Mo–CO stretching ($\nu_8$) and Mo–CO bend ($\nu_7$) modes of adsorbed $Mo(CO)_6$, respectively, in accordance with the vibrational modes for $Mo(CO)_6$ molecules in the gas phase [36–38] and adsorbed on Si(1 1 1) [39], Cu(1 1 1) [30], graphite and Ag(1 1 1) [28]. No distinguished combinative losses, as observed in the case of $Mo(CO)_6$ adsorption on thin alumina film [18], were detected. This suggests that a thick physically adsorbed layer of $Mo(CO)_6$ is not formed under this experimental condition, agreeing well with previous TDS results [13]. These three vibrations simultaneously shift downward in frequency with increasing sample temperature up to 200 K. Upon annealing at 200 K, the C–O stretching mode is located at 2103 $cm^{-1}$. This indicates that chemisorbed $Mo(CO)_6$ undergoes partial decomposition upon annealing. Ho and coworkers also observed the downward shift of the vibrational frequency when adsorbed $Mo(CO)_6$ partially decomposed upon irradiation of photons [28,30]. When the surface was further annealed at 250 K, the C–O stretching mode shifts upward to 2136 $cm^{-1}$, meanwhile, the doublet for the Mo–CO vibrations (the vibrational peaks for Mo–CO stretching and bend modes) in adsorbed $Mo(CO)_6$ disappears. Instead, a single peak emerges at ca. 444 $cm^{-1}$. In comparison with the HREEL spectrum of CO adsorbed on Pt(1 1 0) [13], the vibrational features at 2136 and 444 $cm^{-1}$ could be reasonably assigned to the C–O and Pt–CO stretching vibrations, respectively. This illustrates that adsorbed

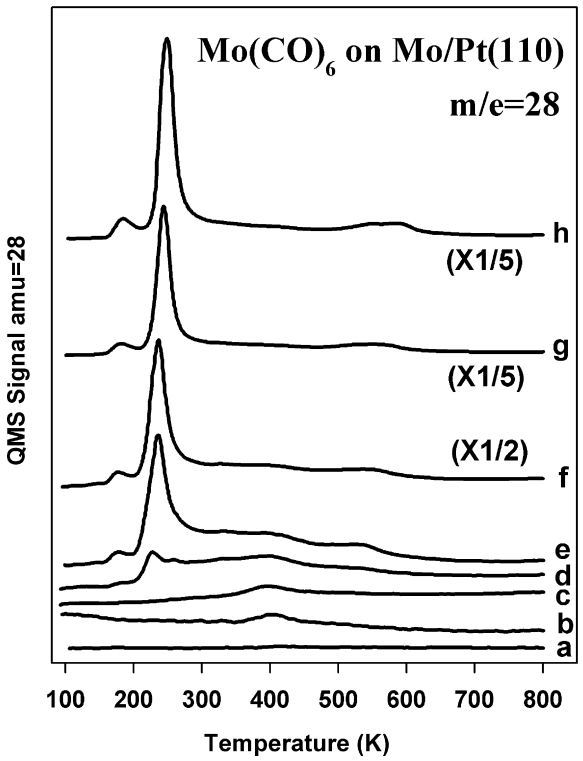


**Fig. 2.** Thermal desorption spectra from the Mo/Pt(1 1 0) model surface with $Mo(CO)_6$ exposure of (a) 0 L, (b) 0.1 L, (c) 0.2 L, (d) 1.0 L, (e) 1.5 L, (f) 2.5 L, (g) 5.0 L, and (h) 10 L.

$Mo(CO)_6$ has fulfilled desorption and/or thermal decomposition upon annealing at 250 K. The appearance of the vibrational features at 444 and 2136 $cm^{-1}$ clearly indicates molecular adsorption of CO on the clean Pt(1 1 0) surface. The C–O stretching vibration exhibits one single feature at such high frequency of 2136 $cm^{-1}$ in HREELS, clearly revealing that only one kind of CO is bonded to the top sites. This is in accordance with the results in literature [40], where CO chemisorption exhibited one loss signal on Pt(1 1 0), while two separate peaks on Pt(1 1 1). Neither bridge bonded CO nor any other adsorption site were detected on Pt(1 1 0), in good agreement with Sharma et al., who reported that CO occupied top sites on Pt(1 1 0) at all coverages and temperatures from 90 to 300 K [41]. With further increasing sample temperatures, the vibrational peaks of CO adsorbed on Pt(1 1 0) attenuate and eventually disappear upon annealing at 600 K. These observations agree well with the previous TDS results showing the desorption feature of 28 amu from the $Mo(CO)_6$-exposed Pt(1 1 0) surface at between 300 and 600 K [13].

Therefore, molybdenum deposition on Pt(1 1 0) could be achieved via thermal decomposition of $Mo(CO)_6$. We prepared a Mo/Pt(1 1 0) model surface by dosing $Mo(CO)_6$ at 700 K followed by annealing at 1000 K, without any carbon and oxygen contaminants [13]. The AES result demonstrates a Mo:Pt atomic ratio of 0.068. This only presents the amount of metallic molybdenum on the employed Mo/Pt(1 1 0) model surface. Since Auger electron spectroscopy penetrates several layers within the sample, the real surface molybdenum coverage is slightly higher, but not far higher, than the value of the surface molybdenum measured by AES. Fig. 2 shows a series of thermal desorption spectra for 28 amu when $Mo(CO)_6$ was dosed to the Mo/Pt(1 1 0) model surface at 100 K. At small exposures, a desorption feature develops at ~406 K, and grows and slightly shifts toward lower temperature with increasing $Mo(CO)_6$ exposure. This peak could be attributed to the desorption of CO formed by thermal decomposition of adsorbed $Mo(CO)_6$ on the Mo/Pt(1 1 0) surface. When the exposure of $Mo(CO)_6$ reaches 1.0 L, a major new peak emerges at 225 K. This feature continuously grows with increasing $Mo(CO)_6$ exposure and does not saturate under the employed conditions, meanwhile, the desorption maximum of the peak shifts upward in desorption temperature with further increasing $Mo(CO)_6$ exposure. This peak is due to molecular desorption of $Mo(CO)_6$ multilayers from platinum sites on the model surface, similar to previous reports [13,33,39]. We also observed other new TDS features at approximately 180 and 540 K, when 1.5 L $Mo(CO)_6$ was dosed onto the Mo/Pt(1 1 0) model surface at 100 K. The feature at 180 K appears in the TDS after the emergence of the peak at 225 K as a function of $Mo(CO)_6$ dosage, and does not exhibit a sign of saturation with increasing $Mo(CO)_6$ exposure. Therefore, this feature must be related with $Mo(CO)_6$ multilayers onto the Mo/Pt(1 1 0) model surface. On clean Pt(1 1 0), there is also the desorption feature at 180 K in the TDS profile; however, it only appears when 3.0 L $Mo(CO)_6$ was dosed onto the Pt(1 1 0) at 100 K, after all desorption experiments of $Mo(CO)_6$ exposure below 3.0 L were performed [13]. Additionally, there must be some molybdenum clusters remaining on the substrate after a cycle of thermal desorption at an intermediate $Mo(CO)_6$ exposure, due to thermal decomposition of molybdenum carbonyl. Accordingly, the feature at 180 K might arise from the desorption of $Mo(CO)_6$ multilayers from some minor sites other than Pt, for example, the residual molybdenum clusters on the model surface. $Mo(CO)_6$ desorption from a polycrystalline Mo surface exhibited a desorption feature at 160–180 K, and the desorption maximum shifted toward higher temperature with increasing $Mo(CO)_6$ exposure [11]. The desorption peak for $Mo(CO)_6$ occurred between 160 and 190 K on Mo(1 0 0), and suggested zero-order desorption [42]. The desorption feature at 540 K is alike assigned to the desorption of CO from the sites except platinum.

Fig. 3 illustrates a series of HREEL spectra of $Mo(CO)_6$ with an exposure of 10 L adsorbed on the Mo/Pt(1 1 0) surface at 100 K and subsequently annealed to the indicated temperatures. A minor

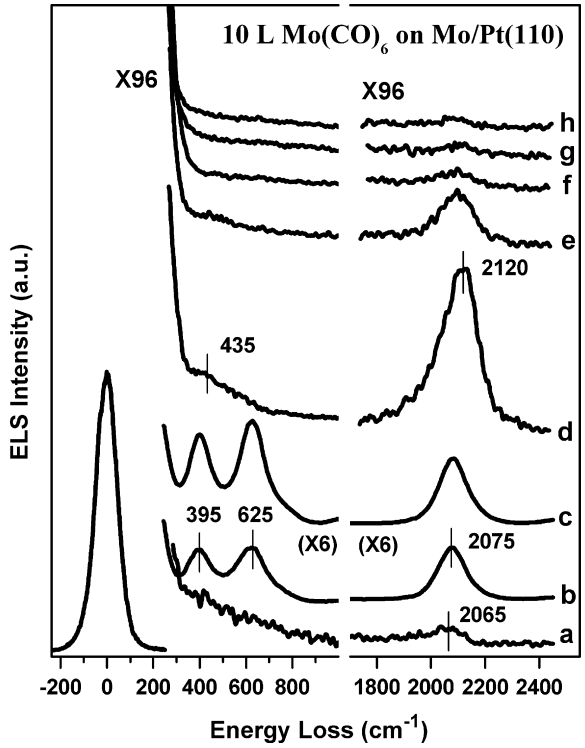


**Fig. 3.** HREEL spectra of (a) a Mo/Pt(1 1 0) model surface at 100 K, then (b) exposed to 10 L $Mo(CO)_6$ at 100 K and subsequently annealed at (c) 200 K, (d) 300 K, (e) 400 K, (f) 500 K, (g) 600 K, and (h) 700 K.

vibrational feature, arising from the adsorption of CO from the background, was observed at ca. 2065 $cm^{-1}$ on the clean Mo/Pt(1 1 0) alloy surface. After an exposure of 10 L $Mo(CO)_6$, an intense signal emerges at 2075 $cm^{-1}$ in the HREELS, accompanied with two intense vibrations at 395 and 625 $cm^{-1}$. Again, these peaks could be assigned to the C–O stretching ($\nu_6$), Mo–CO stretching ($\nu_8$) and Mo–CO bend ($\nu_7$) modes of adsorbed $Mo(CO)_6$, respectively. As compared to those on the clean Pt(1 1 0) surface, the C–O and Mo–CO stretching vibrations of $Mo(CO)_6$ on Mo/Pt(1 1 0) shift downward by a relatively large magnitude. These vibrational frequency downshifts clearly indicate that the reactivity of Pt(1 1 0) toward $Mo(CO)_6$ is greatly modified by the deposited metallic molybdenum. Ho and coworkers reported that partial decomposition of adsorbed $Mo(CO)_6$ led to the downward shift of its vibrational frequencies [28,30]. The C–O stretching feature moved from 2000 to 1984 $cm^{-1}$ when molecularly adsorbed $Mo(CO)_6$ on Ag(1 1 1) and the basal plane of graphite underwent photodissociation [28]. Therefore, the observed large vibrational frequency downshifts on Mo/Pt(1 1 0) might be due to the partially dissociative adsorption of $Mo(CO)_6$, resulting in the formation of molybdenum subcarbonyls, i.e., $Mo(CO)_6$ adsorbs both molecularly and dissociatively on Mo/Pt(1 1 0) at 100 K. Unfortunately, we do not observe simultaneous emergence of two vibrational features with different frequencies for both molecularly and dissociatively adsorbed molybdenum carbonyls in HREELS data, due to the low resolution (~100 $cm^{-1}$). These three vibrational features do not shift when the surface was annealed at 200 K; however, with further increasing annealing temperature to 300 K, the C–O stretching mode shifts upward to 2120 $cm^{-1}$ and the doublet for the Mo–CO vibrations disappears. Instead, a weak peak emerges at approximately 435 $cm^{-1}$. This illustrates that adsorbed $Mo(CO)_6$ and molybdenum subcarbonyls have fulfilled desorption and/or thermal decomposition upon annealing at 300 K. Similar to the case on clean Pt(1 1 0), the vibrational peaks at 435 and 2120 $cm^{-1}$ are both associated with CO adsorbed on the Mo/Pt(1 1 0) surface. This also indicates that one kind of CO is bonded to the top sites on the Mo/Pt(1 1 0) model surface. The M–CO stretching frequency on the Pt(1 1 0) is higher than that on the Mo/Pt(1 1 0) surface, in good agreement with the results of CO chemisorption on Pt(1 1 0) and Mo/Pt(1 1 0) at room temperature [13]. With further increasing sample temperature, the vibrational feature of CO adsorbed on Mo/Pt(1 1 0) decreases its intensity, and eventually disappears.

It has been demonstrated that oxidation of deposited metallic molybdenum on Au(1 1 1) could form the surface $MoO_x$ nanoclusters [43–48]. We oxidized the Mo/Pt(1 1 0) surface at 1000 K in $5.0 \times 10^{-6}$ mbar of $O_2$ for 30 min and acquired a $MoO_x$/Pt(1 1 0) model surface, as evidenced by the appearance of the phonon losses in HREELS [13]. The resulting $MoO_x$ spreads over the model surface, because of monolayer dispersion property of molybdenum oxide upon annealing. The surface coverage of the $MoO_x$ on $MoO_x$/Pt(1 1 0) is a little larger than that of the molybdenum on Mo/Pt(1 1 0) at the same deposit amount. However, it does not completely cover the platinum substrate. When CO was dosed onto the $MoO_x$/Pt(1 1 0) model surface at room temperature, a desorption feature of CO with a considerable intensity appears in the TDS, which can be attributed to CO desorption from the platinum substrate [13]. Fig. 4 displays a series of thermal desorption spectra for 28 amu when $Mo(CO)_6$ was dosed to the $MoO_x$/Pt(1 1 0) model surface at 100 K. A desorption feature develops at ~250 K with a long tail when the $Mo(CO)_6$ exposure is low. With increasing $Mo(CO)_6$ exposure, this peak increases its intensity and slightly shifts toward lower temperature. We assigned this peak mainly to the molecular desorption of $Mo(CO)_6$ monolayer adsorbed on $MoO_x$/Pt(1 1 0). The desorption spectra of $Mo(CO)_6$ adsorbed on $MoO_x$/Pt(1 1 0) at low exposures are completely different from those on Pt(1 1 0) and Mo/Pt(1 1 0), indicating a significant modification effect of the

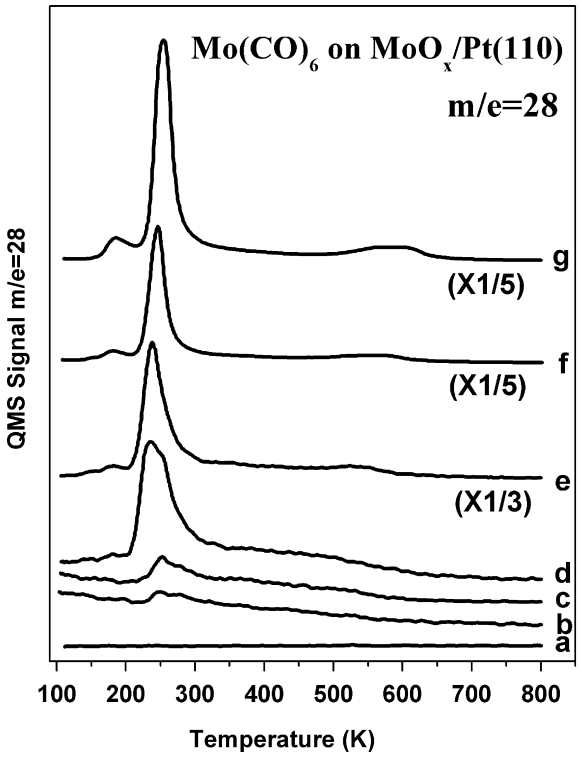


**Fig. 4.** Thermal desorption spectra from the $MoO_x$/Pt(1 1 0) model surface with $Mo(CO)_6$ exposure of (a) 0 L, (b) 0.2 L, (c) 0.3 L, (d) 1.0 L, (e) 2.0 L, (f) 5.0 L, and (g) 10 L.

$MoO_x$ on Pt(1 1 0). With further increasing $Mo(CO)_6$ exposure, the 250 K peak continues to increase its intensity and gradually shifts toward higher temperature. Here this feature at large $Mo(CO)_6$ exposures is mainly contributed from the desorption of adsorbed $Mo(CO)_6$ multilayer. On the $MoO_x$/Pt(1 1 0) model surface, the desorption temperature for $Mo(CO)_6$ multilayer is so close to that for $Mo(CO)_6$ monolayer. It demonstrates that weak interactions occur between adsorbed $Mo(CO)_6$ and $MoO_x$/Pt(1 1 0) at small $Mo(CO)_6$ doses. This indicates that the $MoO_x$ physically blocks the adsorption sites on Pt(1 1 0), consequently inducing the $MoO_x$/Pt(1 1 0) inert toward $Mo(CO)_6$ decomposition. This further confirms the modification effect of the $MoO_x$ on Pt(1 1 0). Similar to the case of Mo/Pt(1 1 0), two new desorption peaks were also observed at approximately 180 and 540 K.

Fig. 5 presents a series of HREEL spectra of $Mo(CO)_6$ with an exposure of 10 L adsorbed on the $MoO_x$/Pt(1 1 0) surface at 100 K and subsequently annealed to the indicated temperatures. The clean $MoO_x$/Pt(1 1 0) surface exhibits two strong vibrational features at 620 and 930 $cm^{-1}$, and a relatively weak and broad signal centered at about 1730 $cm^{-1}$, corresponding to the phonon losses of the $MoO_x$ [13]. After an exposure of 10 L $Mo(CO)_6$, an intense signal emerges at 2120 $cm^{-1}$ in the HREELS, accompanied with two intense vibrations at 405 and 635 $cm^{-1}$. These peaks correspond to the C–O stretching ($\nu_6$), Mo–CO stretching ($\nu_8$) and Mo–CO bend ($\nu_7$) modes of adsorbed $Mo(CO)_6$, respectively. The C–O stretching mode of adsorbed $Mo(CO)_6$ is located at 2120 $cm^{-1}$ on the $MoO_x$/Pt(1 1 0) model surface upon 10 L exposure, close to that at 2130 $cm^{-1}$ on clean Pt(1 1 0) upon 1.0 L exposure. The slight downward frequency shift of the C–O stretching mode is probably caused by different $Mo(CO)_6$ exposures. This clearly suggests that similar surface chemistries of $Mo(CO)_6$ occur on $MoO_x$/Pt(1 1 0) and clean Pt(1 1 0), molecular adsorption at 100 K. These three vibrations all remain almost the same in frequency with slightly increasing sample temperature. When the sample was heated up to 250 K, the C–O stretching mode shifts upward to 2161 $cm^{-1}$ and the doublet for the

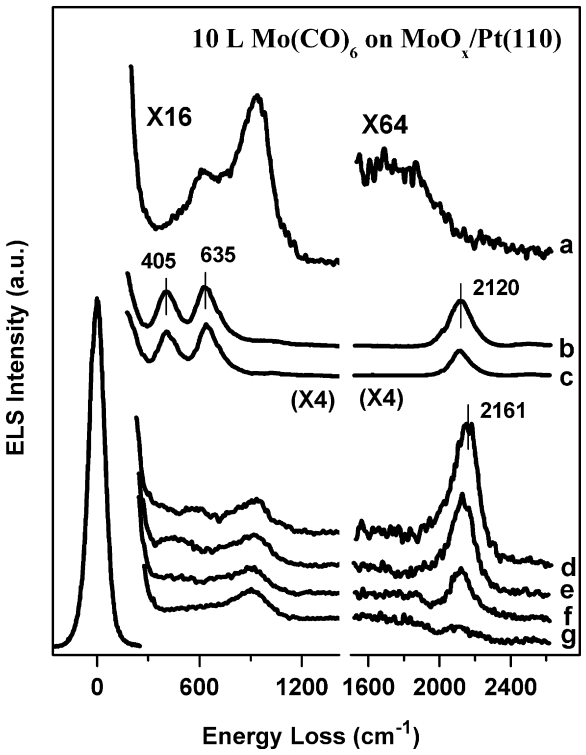


**Fig. 5.** HREEL spectra of (a) a $MoO_x$/Pt(1 1 0) model surface at 100 K, then (b) exposed to 10 L $Mo(CO)_6$ at 100 K and subsequently annealed at (c) 200 K, (d) 250 K, (e) 300 K, (f) 400 K, and (g) 500 K.

Mo–CO vibrations disappears, and the strong phonon losses due to the $MoO_x$ re-appear. This illustrates that adsorbed $Mo(CO)_6$ has fulfilled desorption and/or thermal decomposition upon annealing at 250 K. This C–O vibration at 2161 $cm^{-1}$ is attributed to CO adsorbed on $MoO_x$/Pt(1 1 0). The observed C–O stretching frequency is higher than that of the gas phase value of 2143 $cm^{-1}$. This blue shift is typical for CO adsorbed on $MoO_x$ oxide surfaces and is mainly due to the electrostatic Stark effect. The vibrational Stark effect can be described as a perturbation of the energy of vibrational transitions due to the presence of an electrostatic field; it largely originates from additional anharmonicity that is created within molecular bonds by the presence of the electrostatic field, in which the bond is both mechanically and electronically distorted from equilibrium [49–51]. Since an adsorbed molecule is oriented with respect to the electrostatic field, if it has a static dipole moment then it has a first-order vibrational Stark effect [52]: the induced frequency shift is proportional to the strength of the electrostatic field. The bonding of CO on the $MoO_x$ is largely determined by the electrostatic field strength produced by molybdenum cations in $MoO_x$, consequently affecting carbonyl stretching frequencies of CO coordinated on $MoO_x$. The vibrational Stark effect has recently been employed by Boxer's group to measure the effect of an external electrostatic field on the vibrational spectrum of a molecule via the use of infrared probes [51,53–55]. This technique gives quantitative information on the sensitivity of a vibrational peak position to an electric field. The annealing experiments show that adsorbed CO desorbs from the surface below 500 K. However, it could be seen that the phonon loss peaks of the $MoO_x$ after the entire desorption of adsorbed CO from $MoO_x$/Pt(1 1 0) is much weaker than those prior to the $Mo(CO)_6$ exposure. This clearly demonstrates that some molecularly adsorbed $Mo(CO)_6$ decomposes during the course of heating, forming deposits remaining on the surface. These deposits might be the adsorption sites for the new desorption peaks observed at approximately 180 and 540 K in the TDS upon large $Mo(CO)_6$ exposures.

Above results demonstrate that $Mo(CO)_6$ molecularly chemisorbs on the clean Pt(1 1 0) and $MoO_x$/Pt(1 1 0) surfaces at cryogenic temperature, however, undergoes partial dissociation on the Mo/Pt(1 1 0) surface. Upon heating, these species undergo both molecular desorption and thermal decomposition, forming adsorbed CO and molybdenum clusters on the surface. Inferred from the C–O stretching frequency of adsorbed CO, we can draw the conclusion that the Mo/Pt(1 1 0) surface more strongly donates electrons to adsorbed CO than the Pt(1 1 0) and $MoO_x$/Pt(1 1 0) surfaces. Previous results reported that $Mo(CO)_6$ molecularly chemisorbed on the clean Cu(1 1 1) and Si(1 1 1)-7 × 7 surfaces but dissociatively chemisorbed after these two surfaces were modified by K [30,32]. This indicates that an electron rich surface facilitates the decomposition of $Mo(CO)_6$. The Mo/Pt(1 1 0) surface more strongly donates electrons than the Pt(1 1 0) and $MoO_x$/Pt(1 1 0) surfaces, thus exhibits a higher reactivity toward $Mo(CO)_6$ than the Pt(1 1 0) and $MoO_x$/Pt(1 1 0) surfaces. On the basis of these results, we propose that the interaction of CO ligands in $Mo(CO)_6$ with the substrate determines the adsorption behavior of $Mo(CO)_6$. The dissociation process can be viewed as a competition between central molybdenum atoms and substrate atoms in CO binding. Similar viewpoint in the thermal dissociation process was proposed by Ying and Ho [30], in an attempt to explain the observation of nondissociative adsorption of $Mo(CO)_6$ on Cu(1 1 1) at 85 K and subsequent dissociation at higher temperatures. The stronger the interaction is, the easier $Mo(CO)_6$ dissociatively chemisorbs. CO interacts with Mo/Pt(1 1 0) more strongly than with Pt(1 1 0) and $MoO_x$/Pt(1 1 0), therefore some $Mo(CO)_6$ occurs dissociative adsorption on Mo/Pt(1 1 0). This competition process could be a thermodynamic effect, not a kinetic effect.

Molecular desorption and thermal dissociation are competitive for adsorbed $Mo(CO)_6$ on the surfaces during the course of heating, which primarily depends on $Mo(CO)_6$ coverage, heating rate, and the chemical property of the substrates. The branching ratio between desorption and dissociation was observed to depend on the initial coverage of $Mo(CO)_6$, and the dissociation channel competed favorably with the molecular desorption channel at low $Mo(CO)_6$ exposures [30]. It was reported that slow heating would leave a significant amount of molybdenum on the substrate whereas rapid heating (5–10 K/s) could reduce this amount to about only one-tenth [11,42]. In an attempt to illustrate the modification effect of the deposited metallic molybdenum and $MoO_x$ on the reactivity toward $Mo(CO)_6$, the desorption features with three representative $Mo(CO)_6$ exposures (0.2, 1.0 and 10 L) on clean Pt(1 1 0), Mo/Pt(1 1 0) and $MoO_x$/Pt(1 1 0) were chosen for comparison. When 0.2 L $Mo(CO)_6$ was dosed onto Pt(1 1 0), a major feature appears at approximately 512 K in the TDS, with a shoulder peak at about 260 K. The former is ascribed to thermal decomposition of the adsorbates, and the latter to molecular desorption of $Mo(CO)_6$. The same exposure on Mo/Pt(1 1 0) only gives rise to one desorption feature at 397 K, corresponding to thermal decomposition of the adsorbates upon heating. No molecular desorption of adsorbed $Mo(CO)_6$ is observed, demonstrating a complete thermal dissociation of 0.2 L $Mo(CO)_6$ on Mo/Pt(1 1 0) upon heating. This again evidences a much higher reactivity of Mo/Pt(1 1 0) toward $Mo(CO)_6$ than Pt(1 1 0) because Mo/Pt(1 1 0) more strongly donates electrons than Pt(1 1 0). When 0.2 L $Mo(CO)_6$ was exposed to $MoO_x$/Pt(1 1 0), only one desorption feature centered at 260 K emerges in the TDS profile, corresponding to molecular desorption of adsorbed $Mo(CO)_6$, indicating a weaker interaction of $Mo(CO)_6$ with $MoO_x$/Pt(1 1 0) than with Pt(1 1 0). The integrated intensities of the TDS peaks for 28 amu on Mo/Pt(1 1 0) and $MoO_x$/Pt(1 1 0) are much smaller than that on Pt(1 1 0), which could be attributed to a physically site-blocking effect of the deposits on the platinum substrate. This implies that adsorption sites on Mo/Pt(1 1 0) and $MoO_x$/Pt(1 1 0) are still mainly Pt.

When 1.0 L $Mo(CO)_6$ was dosed onto these three surfaces, both molecular desorption and thermal decomposition of adsorbed $Mo(CO)_6$ occur upon heating, but the branching ratios of molecular desorption to thermal decomposition are different: lowest on Mo/Pt(1 1 0) and highest on $MoO_x$/Pt(1 1 0). These experimental results further validate that Mo/Pt(1 1 0) surface is most active and $MoO_x$/Pt(1 1 0) most inert in thermally decomposing chemisorbed $Mo(CO)_6$. The integrated desorption peak intensities on Mo/Pt(1 1 0) and $MoO_x$/Pt(1 1 0) are still much smaller than that on the clean Pt(1 1 0) surface. When 10 L $Mo(CO)_6$ was dosed, molecular desorption of adsorbed $Mo(CO)_6$ dominates the TDS profiles, clearly indicating the formation of thick physically adsorbed layers on the substrates. The desorption intensities are of the similar magnitude.

## 4. Conclusions

In summary, $Mo(CO)_6$ adsorption was comparatively investigated on Pt(1 1 0), Mo/Pt(1 1 0) and $MoO_x$/Pt(1 1 0) surfaces. $Mo(CO)_6$ adsorbs molecularly on clean Pt(1 1 0) and $MoO_x$/Pt(1 1 0), and partially dissociatively on Mo/Pt(1 1 0) at 100 K. During the course of heating, chemisorbed $Mo(CO)_6$ undergoes molecular desorption and thermal dissociation. The Mo/Pt(1 1 0) surface more strongly donates electrons to adsorbates than the Pt(1 1 0) and $MoO_x$/Pt(1 1 0) surfaces, and thus exhibits a higher reactivity toward $Mo(CO)_6$. We propose that the interaction of CO ligands in $Mo(CO)_6$ with the metal surface determines the adsorption behavior of $Mo(CO)_6$. Our work enriches the surface chemistry of $Mo(CO)_6$ on metallic substrates.

## Acknowledgements

We are grateful for the financial support of the National Natural Science Foundation of China (20773113 and 20803072), Hundred Talent program of Chinese Academy of Sciences, MOE program for PCSIRT (IRT0756) and MPG-CAS partner-group program.

## References

[1] R. Psaro, S. Recchia, Catal. Today 41 (1998) 139.
[2] C. Brémard, Coord. Chem. Rev. 178–180 (1998) 1647.
[3] F. Zaera, J. Phys. Chem. 96 (1992) 4609.
[4] M.D. Xu, F. Zaera, J. Vac. Sci. Technol. A 14 (1996) 415.
[5] F. Zaera, Langmuir 7 (1991) 1188.
[6] F. Zaera, Surf. Sci. 255 (1991) 280.
[7] M.D. Xu, F. Zaera, Surf. Sci. 315 (1994) 40.
[8] F. Zaera, J. Vac. Sci. Technol. A 7 (1989) 640.
[9] M.B. Logan, R.F. Howe, R.P. Cooney, J. Mol. Catal. 74 (1992) 285.
[10] S.D. Djajanti, R.F. Howe, Stud. Surf. Sci. Catal. 97 (1995) 197.
[11] C.C. Cho, S.L. Bernasek, J. Appl. Phys. 65 (1989) 3035.
[12] Z.Q. Jiang, W.X. Huang, J. Jiao, H. Zhao, D.L. Tan, R.S. Zhai, X.H. Bao, Appl. Surf. Sci. 229 (2004) 43.
[13] Z.Q. Jiang, W.X. Huang, H. Zhao, Z. Zhang, D.L. Tan, X.H. Bao, J. Mol. Catal. A 268 (2007) 213.
[14] M. Kurhinen, T. Venäläinen, T.A. Pakkanen, J. Phys. Chem. 98 (1994) 10237.
[15] C.C. Williams, J.G. Ekerdt, J. Phys. Chem. 97 (1993) 6843.
[16] R.-I. Nakamura, R.G. Bowman, R.L. Burwell, J. Am. Chem. Soc. 103 (1981) 673.
[17] R.-I. Nakamura, D. Pioch, R.G. Bowman, R.L. Burwell, J. Catal. 93 (1985) 388.
[18] Z.Q. Jiang, W.X. Huang, Z. Zhang, H. Zhao, D.L. Tan, X.H. Bao, Surf. Sci. 601 (2007) 844.
[19] M. Kaltchev, W.T. Tysoe, J. Catal. 193 (2000) 29.
[20] M. Kaltchev, W.T. Tysoe, J. Catal. 196 (2000) 40.
[21] M. Kaltchev, W.T. Tysoe, Top. Catal. 13 (2000) 121.
[22] Y. Wang, F. Gao, M. Kaltchev, D. Stacchiola, W.T. Tysoe, Catal. Lett. 91 (2003) 83.
[23] Y. Wang, F. Gao, M. Kaltchev, W.T. Tysoe, J. Mol. Catal. A 209 (2004) 135.
[24] Y. Wang, F. Gao, W.T. Tysoe, J. Mol. Catal. A 235 (2005) 173.
[25] Y. Wang, F. Gao, W.T. Tysoe, J. Mol. Catal. A 248 (2006) 32.
[26] T.A. Germer, W. Ho, J. Chem. Phys. 89 (1988) 562.
[27] T.A. Germer, W. Ho, J. Vac. Sci. Technol. A 7 (1989) 1878.
[28] S.K. So, W. Ho, J. Chem. Phys. 95 (1991) 656.
[29] H.H. Huang, C.S. Sreekanth, C.S. Seet, X. Jiang, G.Q. Xu, Surf. Sci. 365 (1996) 769.
[30] Z.C. Ying, W. Ho, J. Chem. Phys. 93 (1990) 9077.
[31] Z.C. Ying, W. Ho, J. Chem. Phys. 94 (1991) 5701.
[32] D.V. Chakarov, Z.C. Ying, W. Ho, Surf. Sci. 255 (1991) L550.
[33] Z.C. Ying, W. Ho, Phys. Rev. Lett. 65 (1990) 741.
[34] Z.Q. Jiang, W.P. Zhou, D.L. Tan, R.S. Zhai, X.H. Bao, Surf. Sci. 565 (2004) 269.
[35] Z.Q. Jiang, W.X. Huang, D.L. Tan, R.S. Zhai, X.H. Bao, Surf. Sci. 600 (2006) 4860.
[36] L.H. Jones, Spectrochim. Acta 19 (1963) 329.
[37] L.H. Jones, J. Chem. Phys. 36 (1962) 2375.
[38] L.H. Jones, R.S. McDowell, M. Goldblatt, Inorg. Chem. 8 (1969) 2349.
[39] C.E. Bartosch, N.S. Gluck, W. Ho, Z. Ying, Phys. Rev. Lett. 57 (1986) 1425.
[40] H. von Schenck, E. Janin, O. Tjernberg, M. Svensson, M. Göthelid, Surf. Sci. 526 (2003) 184.
[41] R.K. Sharma, W.A. Brown, D.A. King, Surf. Sci. 414 (1998) 68.
[42] C.C. Cho, S.L. Bernasek, J. Vac. Sci. Technol. A 5 (1987) 1088.
[43] Z.P. Chang, Z. Song, G. Liu, J.A. Rodriguez, J. Hrbek, Surf. Sci. 512 (2002) L353.
[44] Z. Song, T.H. Cai, Z.P. Chang, G. Liu, J.A. Rodriguez, J. Hrbek, J. Am. Chem. Soc. 125 (2003) 8059.
[45] M.M. Biener, J. Biener, R. Schalek, C.M. Friend, J. Chem. Phys. 121 (2004) 12010.
[46] M.M. Biener, C.M. Friend, Surf. Sci. 559 (2004) L173.
[47] S.Y. Quek, M.M. Biener, J. Biener, C.M. Friend, E. Kaxiras, Surf. Sci. 577 (2005) L71.
[48] X.Y. Deng, S.Y. Quek, M.M. Biener, J. Biener, D.H. Kang, R. Schalek, E. Kaxiras, C.M. Friend, Surf. Sci. 602 (2008) 1166.
[49] D.M. Bishop, J. Chem. Phys. 98 (1993) 3179.
[50] N.S. Hush, J.R. Reimers, J. Phys. Chem. 99 (1995) 15798.
[51] S.S. Andrews, S.G. Boxer, J. Phys. Chem. A 106 (2002) 469.
[52] D.K. Lambert, Phys. Rev. Lett. 50 (1983) 2106;
D.K. Lambert, Phys. Rev. Lett. 51 (1983) 2233 (E).
[53] G.U. Bublitz, S.G. Boxer, Ann. Rev. Phys. Chem. 48 (1997) 213.
[54] I.T. Suydam, C.D. Snow, V.S. Pande, S.G. Boxer, Science 313 (2006) 200.
[55] L.J. Webb, S.G. Boxer, Biochemistry 47 (2008) 1588.